Stochastic tool wear assessment in milling difficult to machine alloys

Farbod Akhavan Niaki*

International Center for Automotive Research,
Clemson University,
Greenville, SC, USA
Email: fakhava@clemson.edu
*Corresponding author

Durul Ulutan

Mechanical Engineering Department,
Bucknell University,
Lewisburg, PA, USA
Email: du005@bucknell.edu

Laine Mears

International Center for Automotive Research,
Clemson University,
Greenville, SC, USA
Email: mears@clemson.edu

Abstract: In the machining industry, maximising profit is intuitively a primary goal; therefore continuously increasing machining process uptime and consequently productivity and efficiency is crucial. Tool wear plays an important factor in both machining uptime and quality, and since tool failure is related to the surface quality and the dimensional accuracy of the end product, it is essential to quantify and predict this phenomenon with the best possible certainty. One of the most common ways of tool wear prediction is through the use of low cost spindle current sensing technology which is used to measure spindle power consumption in CNC machines and relate power increase to tool wear. In this work, two methods of stochastic filtering (i.e. Kalman and particle filter) were used in predicting tool flank wear in machining difficult-to-machine materials through spindle power consumption measurements. Results show a maximum of 15% average error in estimation, which indicates the good potential of using stochastic filtering techniques in estimating tool flank wear. In addition, the particle filter was used for online estimation of a spindle power model parameter with uniform and Gaussian mixture models as the initial probability density functions, and the evolution of this parameter to the true posterior density function over time was investigated.

Keywords: tool wear; Kalman filter; particle filter; milling.

Reference to this paper should be made as follows: Akhavan Niaki, F., Ulutan, D. and Mears, L. (2015) 'Stochastic tool wear assessment in milling difficult to machine alloys', *Int. J. Mechatronics and Manufacturing Systems*, Vol. 8, Nos. 3/4, pp.134–159.

Biographical notes: Farbod Akhavan Niaki is a PhD candidate of Automotive Engineering at the Clemson University, International Center for Automotive Research (CU-ICAR). He received his Master's degree from Sharif University of Technology specialising in modelling and simulation of dynamical systems. Since 2013, he joined Informed Control of Manufacturing lab at CU-ICAR working on tool condition monitoring and model based control of manufacturing processes.

Durul Ulutan is an Assistant Professor at Bucknell University, Mechanical Engineering Department. He received his BS (2005) and MS (2007) degrees from Koç University (Turkey), Mechanical Engineering Department, and his PhD degree from the Department of Industrial and Systems Engineering at Rutgers University (2013). After his PhD studies, he worked at Clemson University, International Center for Automotive Research (CU-ICAR) as a Post-Doctoral Researcher. He has over ten years of experience in analysing, modelling, and optimising manufacturing processes and systems.

Laine Mears is Professor and founding faculty member in the Automotive Engineering Department at Clemson University, teaching and carrying out projects at the Clemson University International Center for Automotive Research. He teaches modelling and analysis of automotive manufacturing processes, quality systems and quality tools, and performs research in manufacturing quality systems, intelligent machining systems, manufacturing process design and control, and manufacturing equipment diagnostics. He has published over 100 peer-reviewed articles, and is the recipient of the NSF CAREER award, SAE Ralph Teetor Educational Award, the South Carolina Governor's Young Researcher Award for Excellence in Scientific Research and the IMECHE George Stephenson Gold Medal.

This paper is a revised and expanded version of a paper entitled 'In-process tool flank wear estimation in machining gamma-prime strengthened alloys using Kalman filter' presented at North American Manufacturing Research Conference (NAMRC), Charlotte, NC, USA, 8–12 June 2015.

1 Introduction

In machining processes, one of the main drivers of total cost of production is tool wear and failure. Because of this, monitoring the condition of the cutting tool has been the focus of many researchers recently (Roth et al., 2010). Tool wear is known to be the primary cause of surface quality losses, as well as the health of the machine and the machining downtime (Vallejo et al., 2005). Tool wear has been studied using two different approaches, online (indirect) and offline (direct) methods, and there are benefits and concerns associated with using both methods.

In direct (offline) methods, the process is interrupted for the tool wear measurement via stopping the machine, accessing the tool and utilising a device such as an optical microscope or vision systems (Ertunc et al., 2001; Jeon and Kim, 1988; Pedersen, 1990). Due to its direct nature, the accuracy of the information from these methods is considered to be higher for tool condition monitoring (TCM). However, automated manufacturing systems do not benefit from these methods due to the interruptions to the process as well as the extended time and cost.

In indirect (online) methods, external signals that are merely indicators of tool wear are measured, and the relationship between these signals and tool wear are utilised in order to predict tool failure (Li, 2002; Lin and Yang, 1995; Cuppini et al., 1990; Wang et al., 2002). Such external signals could originate from different sources such as acoustic emission (AE) or vibration sensors as well as machining force and torque via a dynamometer and spindle power consumption via spindle current measurements. The main benefit of these methods is the lack of the need for process interruption; therefore, there is no decrease in productivity. On the other hand, signals from external sources usually bring uncertainty to the analysis, so extracting the relevant features of such signals is another challenge. Finally, appropriate models with good prediction accuracy need to be created to be able to estimate tool wear from these signals. Such models are grouped as: empirical, mechanistic, and dynamic models. Empirical models help researchers understand tool wear by fitting a mathematical function to a set of experimental values (Li, 2002). Mechanistic models are used to relate measured machining forces or spindle power consumption analytically to tool wear through equations derived and validated extensively in time (Fu et al., 1984; Cuppini et al., 1990; Xu et al., 2011). Dynamic models are used by researchers to analyse the progress of tool wear in state space time series models (Danai and Ulsoy, 1987a, 1987b).

Studying tool wear and its evolution in the time domain has been a more common method than study in the frequency domain, since it is relatively easy and well understood. However, researchers have been exploring the frequency domain and the joint time-frequency domain to further the understanding of tool wear. More commonly used techniques of such nature are: machine learning techniques like neural network, support vector method (SVM), hidden Markov model (HMM), and self-organising map (SOM). These methods are mostly used for predicting or categorising tool wear in machining processes such as milling and drilling (Owsley et al., 1997; Ertunc et al., 2001; Wang et al., 2002; Zhu et al., 2009; Xu et al., 2011). The Kalman filter is another method that has shown good noise suppression characteristic and it has been used by some researchers in machining process control (Möhring et al., 2010; Henderson, 2012; Akhavan Niaki et al., 2015a). The Kalman filter works as a low pass optimal filter in linear stochastic systems where states and measurements are corrupted by noise. Since 1960 that the method proposed; other extensions such as extended Kalman filter (EKF) or unscented Kalman filter (UKF) were introduced to stretch the application of stochastic filtering into nonlinear domains (Wan and Van Der Merwe, 2000; Haykin, 2001).

The objective of this study is to investigate the applicability of using stochastic model-based estimation methods (i.e. Kalman filter and Particle filter) in tool wear assessment of hard to machine materials. To emphasise the usability of methods in industrial plants, the low-cost sensing technology, particularly spindle power consumption is selected as online measuring system. Accurate estimation of tool wear is of great importance in automated machining processes to achieve decreased idle time and improved productivity. Two types of stochastic filtering methods, Kalman filter and Particle filter are deployed here for tool wear estimation, and their results are compared. The organisation of this work is as follows: theoretical background of Kalman filter and Particle are discussed in Section 2. Proper mechanistic model for spindle power is explained in Section 3. In Section 4, the experimental setup is explained and selected cutting conditions for experiments are given. In Section 5, stochastic modelling of tool flank wear is discussed. Results and conclusions are provided in Sections 6 to 8.

2 Theoretical background

2.1 Kalman filter

According to the Bayes rule introduced in the 18th century, the multiplication of the initial belief of an event x, denoted $p(x)$ and the observed dataset $p(y \mid x)$ can be divided by the marginal distribution of the observed data $p(y)$ to give the actual probability of the event $p(x \mid y)$, where $p(y)$ can be found using equation (1). This type of prediction helped researchers working on data mining strategies where estimation of the state of event x has been easier via high number of observations. Using the Bayes rule, Rudolf Kálmán introduced a method of estimation where a Gaussian model is assumed for the states of events, and at each recursive time step forward, these states are estimated. In addition, whenever a new measurement becomes available, the estimated states are updated (Kalman, 1960). Methods based on Kalman's idea (Kalman filter) were proposed to remove the system linearity requirement, such as the EKF or the UKF (Haykin, 2001). However, in its most basic formulation, a discrete linear state space equation [equation (2)] is used to define the relationship. The measured signal z_k can be expressed as a discrete stochastic model with a matrix H that relates the current state of the system to the measurements [equation (3)]. The noise expressions w_{k-1} and v_k are defined as normally distributed variables with a mean of zero and variance of Q and R, respectively [equation (4)]. Bayesian estimation was introduced by Thomas Bayes who proposed the basic formulation, known as the Bayes rule, in the 18th century (Hoff, 2009). According to this rule, the probability of an event x – $p(x \mid y)$ – can be derived by multiplying the initial belief (i.e. *a priori*) of x with the observed dataset $p(y \mid x)$, and dividing by the marginal distribution of observed data $p(y)$. This marginal distribution $p(y)$ is derived as shown in equation (1).

$$p(y) = \int p(y \mid x) p(x) dx \tag{1}$$

Bayesian estimation is extensively used in the context of data mining where batch of observations (i.e. measurements) are available to estimate state x. In practical application, having an online estimation of the states or the parameters using a previously established model is of great importance. Using Bayes rule, Rudolf Kálmán coined a recursive estimation method in 1960 (i.e. Kalman filter), which assumes a Gaussian model for states and estimates them at each time step and updates the estimation when a new measurement is available (Kalman, 1960). Since then, the Kalman filter has been extensively used in the area of target tracking and navigation, where a linear behaviour of system is valid. The EKF and the UKF are also proposed for tracking states in nonlinear systems (Haykin, 2001). For state estimation, the Kalman filter uses a discrete linear state space equation [equation (2)], where k is the time step, A is a matrix that relates the states at the previous time step ($k - 1$) to the current time step (k), B is a matrix that relates inputs u at the previous time step to the current states, and w_k is the noise (uncertainty) for states. This noise is assumed to have a normal distribution with zero mean and variance Q [equation (3)]. The measurement equation is described as a discrete stochastic model that relates current state to measured signals [equation (4)], where z_k is the measured signal, H is a matrix that relates current states of system to the most recent measurements and v_k is the measurement noise which is assumed to have a normal distribution with zero mean and variance R.

$$x_k = Ax_{k-1} + Bu_{k-1} + w_{k-1} \tag{2}$$

$$w_k \sim N(0, Q) \tag{3}$$

$$z_k = Hx_k + v_k \tag{4}$$

Assuming an observability of states, the Kalman filter is an optimal observer that minimises the expected value of sum of square errors of x_k given the previous observations. Using the closed loop observer formulation for state estimation [equation (5) with K as observer gain], Kalman filter starts with *a priori* information at time k, which is updated based on the previous knowledge at time $k - 1$. As soon as the measurements become available, *a priori* will be updated to find *a posteriori* of states.

$$\hat{x}_k = A\hat{x}_{k-1} + Bu_{k-1} + K\left(z_k - H\hat{x}_k\right) \tag{5}$$

The first update in the algorithm to find *a priori* is called the time update and the second update to find *a posteriori* is called the measurement update. Because the process is recursive, there is no need to wait for the full set of measurements to be available, just those of the next time step. Time and measurement updates are described as below:

1 time update:

$$\hat{x}_k^- = A_{k-1}\hat{x}_{k-1} + Bu_{k-1} \tag{6}$$

$$P_k^- = A_{k-1}P_{k-1}A_{k-1}^T + Q_{k-1} \tag{7}$$

2 Measurement update:

$$K_k = P_{k-1}^- H_k^T \left(H_k P_{k-1}^- H_k^T + R_k\right)^{-1} \tag{8}$$

$$\hat{x}_k = \hat{x}_k^- + K_k\left(z_k - H_k\hat{x}_k^-\right) \tag{9}$$

$$P_k = \left(I - K_k H_k\right)P_k^- \tag{10}$$

Here, P_k^- is the *a priori* error variance of states, P_k is the *a posteriori* error variance of states, $\hat{x}_k^-$ is the *a priori* estimation of states, $\hat{x}_k$ is the *a posteriori* estimation of states, K_k is the Kalman gain, and R_k is the measurement error variance (Haykin, 2001). Note that when a measurement is not available, only the time update of the Kalman filter will be used. In that case, the current knowledge of states makes future predictions possible. Measurement covariance (R_k) can be calculated by evaluating multiple measurements of the signal z when the system is in static mode. In that case, the calculated measurement covariance is considered as the measurement error covariance R_k. On the other hand, calculating the state noises is not that simple. A suggested solution is where the states can be measured offline; in that case the maximum covariance of multiple offline measurement of states can be considered as the state error covariance Q_k. In the case where states are not available, usually tuning the state covariance matrix by trial and error is suggested to get the best estimation. The Kalman filter algorithm is shown in Figure 1.

Figure 1 Kalman filter algorithm

- (0) Initialise states
  - Choose X_0
  - Choose P_0
- (1) Start with $k = 1$
- (2) Time update
  - Calculate $\hat{x}_k^- = A_{k-1}\hat{x}_{k-1} + Bu_{k-1}$
  - Calculate $P_k^- = A_{k-1}P_{k-1}A_{k-1}^T + Q_{k-1}$
- (3) Kalman gain
  - Calculate $K_k = P_{k-1}^- H_{k-1}^T \left(H_k P_{k-1}^- H_k^T + R_k\right)^{-1}$
- (4) Measurement update
  - Calculate $\hat{x}_k = \hat{x}_k^- + K_k\left(z_k - H_k\hat{x}_k^-\right)$
  - Calculate $P_k = \left(I - K_k H_k\right)P_k^-$
- GO to line (1)

2.2 Sequential Monte Carlo filtering

Monte Carlo (MC) methods are used for drawing samples from posterior distribution of states or parameters. An extension to MC methods based on the recursive process of generating samples to estimate the posterior probability density function (pdf) at each time step is called sequential Monte Carlo (SMC) filtering or Particle filtering. This method was first introduced in 1950, and it has recently gained more attention in state and parameter estimation in manufacturing and chemical processes (Imtiaz et al., 2006; Rawlings and Bakshi, 2006). Similar to the Kalman filter, the target when using the Particle filter is estimating process states or identifying unknown parameters of the system. However, the major difference lies in the fact that the Particle filter generates random samples from an unknown posterior pdf of states, and assigns weights to each sample. The combination of samples and weights characterise the posterior pdf. In addition, it is assumed in the Kalman filter framework that the states, state noises, and measurement noises are characterised by Gaussian distributions, so the knowledge of mean and covariance are sufficient to define them. However, in the Particle filter framework, any arbitrary distribution can be assumed due to the fact that random samples are characterising the posterior pdfs. This feature is particularly useful when the system's behaviour is characterised by non-Gaussian distributions such as bimodal or Gamma distributions; in that case Kalman filter cannot be deployed. Last but not least, the Particle filter can be used for both linear or nonlinear systems.

Assuming a discrete state space representation of a system as shown in equation (2), the objective is to find the posterior pdf of x at time step k conditioned on all the previous measurements. It can be shown that each arbitrary pdf $\pi(x)$ for which it is difficult to draw samples can be estimated by another proposal density function $q(x)$ that can be more easily sampled (Doucet et al., 2001). By drawing enough samples, the pdf of $\pi(x)$

can be estimated as equation (11), where ω_i is the weight calculated using equation (12) for each drawn sample.

$$\pi(x) \approx \sum_{i=1}^{N_s} \omega^i \delta(x - x^i) \tag{11}$$

$$\omega^i \propto \frac{\pi(x^i)}{q(x^i)} \tag{12}$$

It is implied in equation (12) that the larger weights indicate that the drawn samples from the proposal density function are closer to the regions with higher probability of $\pi(x)$. Using the previous available observations $z_{1:k}$, the weights can be written as equation (13) (Arulampalam et al., 2002). Sample weights at each time step can be recursively written as equation (14).

$$\omega_k^i = \frac{p(x_{0:k}^i \mid z_{1:k})}{q(x_{0:k}^i \mid z_{1:k})} \tag{13}$$

$$\omega_k^i \propto \omega_{k-1}^i \frac{p(z_k \mid x_k^i)\, p(x_k^i \mid x_{k-1}^i)}{q(x_k^i \mid x_{k-1}^i, z_k)} \tag{14}$$

The optimal choice of proposal density function q plays an important role in the stability of the method. The optimal choice for the pdf of q can be chosen as equation (15) (Doucet et al., 2001). Assuming independence of the states x_k from the measurement z_k, equation (15) can be rewritten as shown in equation (16)–(17).

$$\left[q(x_k^i \mid x_{k-1}^i, z_k)\right]_{opt} = p(x_k^i \mid x_{k-1}^i, z_k) \tag{15}$$

$$\left[q(x_k^i \mid x_{k-1}^i, z_k)\right]_{opt} = p(x_k^i \mid x_{k-1}^i, z_k) = p(x_k^i \mid x_{k-1}^i) \tag{16}$$

$$\omega_k^i \propto \omega_{k-1}^i p(z_k \mid x_k^i) \tag{17}$$

Note that weights should be normalised after each time step. One of challenges with Particle filtering is called the degeneracy problem, where after a few iterations, the weights of all samples but one approach zero and the algorithm fails to converge. This phenomenon can be overcome by calculating the effective number of generated samples (N_{eff}) and resampling particles according to their weights (Doucet et al., 2001; Arulampalam et al., 2002). The smaller N_{eff} means that more severe degeneracy exists. As shown in Figure 2, after the resampling step, particles with higher weights are reproduced more often than particles with lower weights. A number of methods for resampling exist; however, reviewing all of these methods is not the scope of this work. From the pool of different methods, systematic resampling (Kitagawa, 1996) was chosen and applied in the Particle filter framework. The Particle filter algorithm is shown in Figure 3, and to emphasise the difference between the Kalman and Particle filters, both algorithms are compared in Figure 4 and Figure 5.

Figure 2 Resampling of particles to avoid degeneracy problem

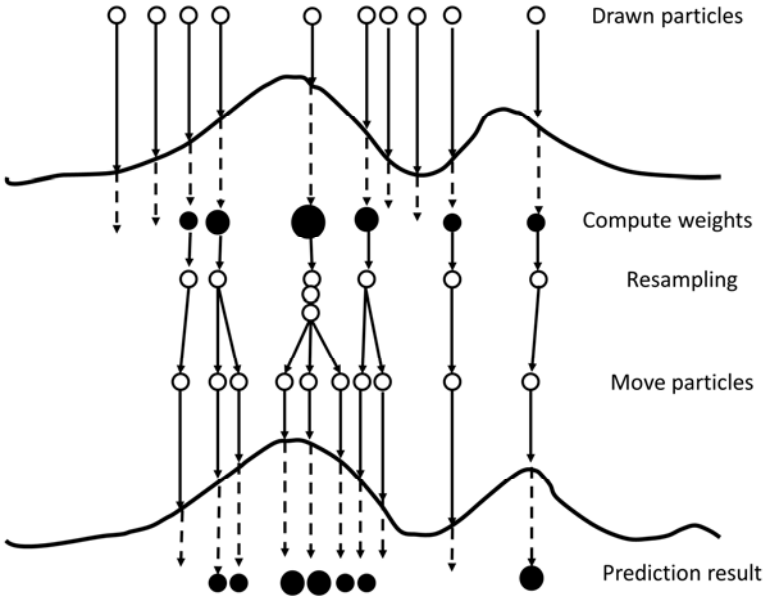

Source: Andrieu et al. (2003)

Figure 3 Particle filter algorithm

- (0) FOR $i = 1{:}N_s$ and $k = 0$
  - Draw sample from prior pdf of $x_0^i \sim p(x_0)$
  - Assign weights $\omega_0^i = \frac{1}{N_s}$
- END FOR
- (1) Start with $k = 1$
- (2) FOR $i = 1{:}N_s$
  - Draw $x_k^i \sim p\left(x_k \mid x_{k-1}^i\right)$
  - Calculate $\omega_k^i = p\left(z_k \mid x_k^i\right)$
- END FOR
- (3) Normalise ω_k^i
- (4) Calculate N_{eff}
- (5) IF $N_{eff} < N_s$
  - Resample with systematic resampling method
  - Replace weights $\omega_k^i = \frac{1}{N_s}$
- END IF
- GO to line (1)

Figure 4 Kalman filter schematic (see online version for colours)

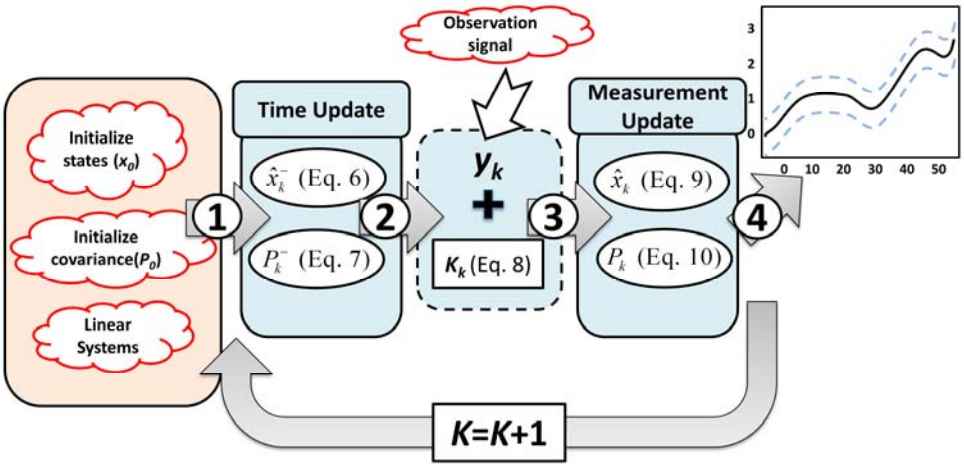

Figure 5 Particle filter schematic (see online version for colours)

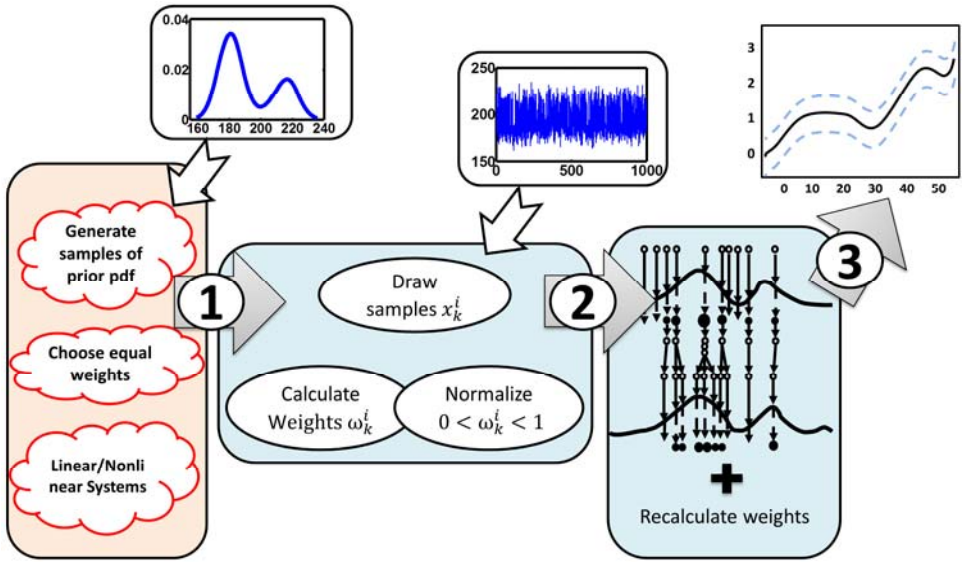

3 Mechanistic tool wear model

It was shown by researchers that the tangential component of the machining force in milling can be formulated as equation (18), where K' and c are constants, $\overline{h}$ is the mean chip thickness, a_p is the depth of cut (mm), f is the feedrate (mm/rev), φ is the instantaneous angle of rotation and F_t is tangential force (N) (Altintas and Yellowley, 1989).

$$F_t = K'\overline{h}^c a_p f \sin\varphi \tag{18}$$

Unlike turning where the uncut chip thickness h can be considered constant, milling induces changing chip thickness with the angle of rotation so that h should be written as a function of the rotational angle, using Figure 6 as schematic of milling. Then, the mean chip thickness $\overline{h}$ can be written in terms of the immersion angles (ψ_1 and ψ_2, respectively) as shown in equation (19). In conventional milling tests, these two angles are usually constant, so equation (19) reduces to equation (20), where m is number of cutter teeth and C_1 is a constant.

$$\overline{h} = \frac{1}{\varphi_{out} - \varphi_{in}} \int_{\varphi_{in}}^{\varphi_{out}} h(\varphi) d\varphi = \frac{1}{m} \frac{1}{\psi_1 + \psi_2} f \left(\sin\psi_1 + \sin\psi_2 \right) \tag{19}$$

$$\overline{h} = C_1 f \tag{20}$$

Figure 6 Milling schematic

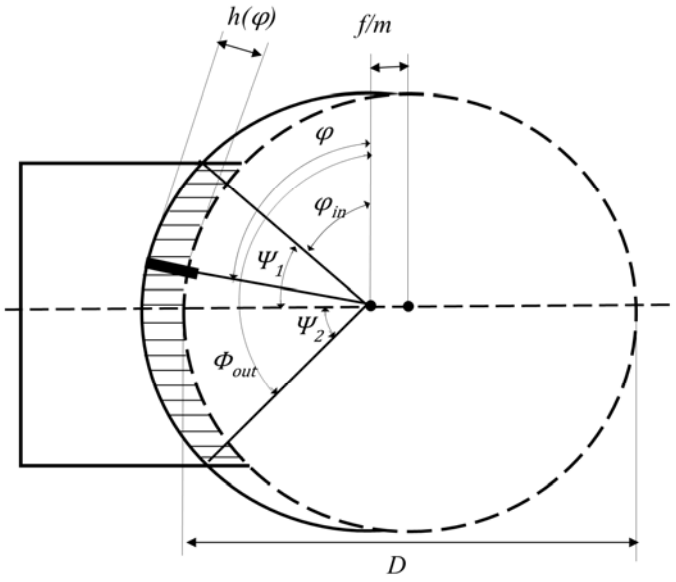

Source: Shao et al. (2004)

It was shown that with an increase in tool wear, the magnitude of force increases as well (Choudhury and Rath, 2000). Also, Waldorf and colleagues showed that the change in magnitude of tangential force F_t^{wear} is a function of the material hardness H_h, the friction coefficient μ, the tool flank wear VB and the tool wear length s represented by equation (21), where s is assumed to be equal to the depth of cut a_p (Shao et al., 2004; Waldorf et al., 1992). All the parameters in equation (21) can be assumed constant in milling except for VB, which changes relative to the volume of material removed in the process. Then, adding equation (18) to equation (21), the resultant tangential force can be written as equation (22), where C_2 is a constant that summarises the constant variables in equation (21).

$$F_t^{wear} = \mu VBH_h s \tag{21}$$

$$F_t = K'C_1' f^{c+1} a_p \sin\varphi + C_2 VB \tag{22}$$

It was also shown by Waldorf et al. (1992) that the constant K' is dependent on cutting conditions including feedrate, and depth of cut [equation (23)], where C_3 is a constant, and α_1 and α_2 are the feedrate and depth of cut exponents, respectively. Plugging equation (23) into equation (22), the tangential force is derived as a function of cutting conditions [equation (24)]. Multiplying the tangential force F_t with the cutter diameter D and spindle speed N yields to instantaneous cutting power P [equation (25)]. With assumption of constant depth of cut in this work, the average power can be simply determined by integrating equation (25) from the entering angle to the exiting angle of the block, and be simply written as shown in equation (26), where K_1 to K_3 are unknown parameters that need to be identified.

$$K' = C_3 f^{\alpha_1} a_p^{\alpha_2} \tag{23}$$

$$F_t = C_1' C_3 f^{c+\alpha_1+1} a_p^{\alpha_2+1} \sin\varphi + C_2 VB \tag{24}$$

$$P = C_1' C_3 D f^{c+\alpha_1+1} N a_p^{\alpha_2+1} \sin\varphi + C_2 DNVB \tag{25}$$

$$P = K_1 N f^{K_2} + K_3 NVB \tag{26}$$

4 Experimental setup

As shown in Figure 7, a total of eight experiments with three replications were conducted in this work to study the tool wear when machining the gamma prime strengthen alloy; Rene-108 (R-108). Among these three replications, the first two were chosen as training sets, and the last replication was chosen for validating the results (i.e. the testing set). Poor thermal conductivity and rapid work hardening make R-108 a hard-to-machine material, so the tool wear rate of inserts during the process is relatively high compared to other conventional materials. High tool wear rate while machining R-108 makes establishing an accurate tool wear model a challenging task because only a limited number of experiments can be completed before the tool fails. In such cases, utilising the prior knowledge about parameters of a model and combining it with the likelihood function makes Bayesian analysis a powerful method when enough experimental results is not available or conducting large number of experiments is costly (Akhavan Niaki et al., 2015b). The alternative is repeating the experiments to eliminate the effect of measurement noises or other undesirable effects induced during machining. That justifies the use of two sets of replications as training sets for initial estimation of the parameters in the model.

Figure 7 Schematic of milling experiments (see online version for colours)

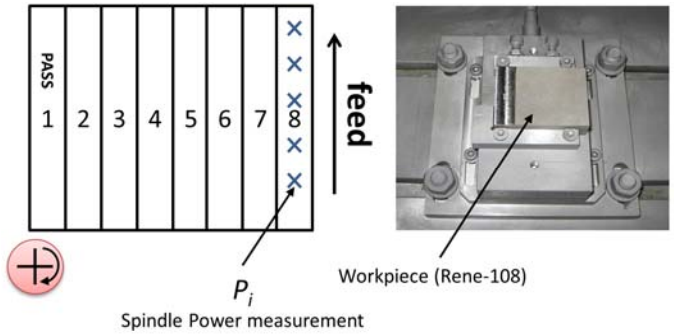

An OKUMA GENOS M460-VE 3-axis CNC machine was used to end mill (in the down-milling direction) rectangular blocks of size 60 × 80 × 25 mm, using a water-soluble coolant. A 2-flute indexable tool holder with a diameter of 15.875 mm was used, and the width of cut was chosen to be 9.5 mm that corresponds to 60% tool engagement, as this was the maximum manufacturer recommendation for the particular tool holder. Full length of the blocks (60 mm) was utilised for machining, which was considered as a 'pass'. At the chosen width of cut, 24 tests were conducted on the block: eight tests with three replications. Depth of cut, cutting velocity and feedrate for each pass are kept constant at 0.5 mm, 25 m/min and 0.1 mm/rev respectively. The cutting conditions are determined based on the industrial applications targeted by this study, and keeping the cutting conditions constant is due to the fact that a change in the cutting conditions can induce abrupt changes in the behaviour of hard-to-machine alloys. Therefore, in order to duplicate the same machining conditions as in industrial applications, these conditions were kept constant. A data acquisition device (DAQ) was programmed to capture the spindle power consumption while cutting with high sampling rate. To measure spindle power in high sampling frequency, the output of the TMAC transducer (Figure 8) was fed into the NI9215 analogue input module mounted on NI-cRIO9103 chassis programmed with LabVIEW. Data was collected at a sampling frequency of 10.24 kHz.

Figure 8 Data acquisition with NI-cRIO9103 (see online version for colours)

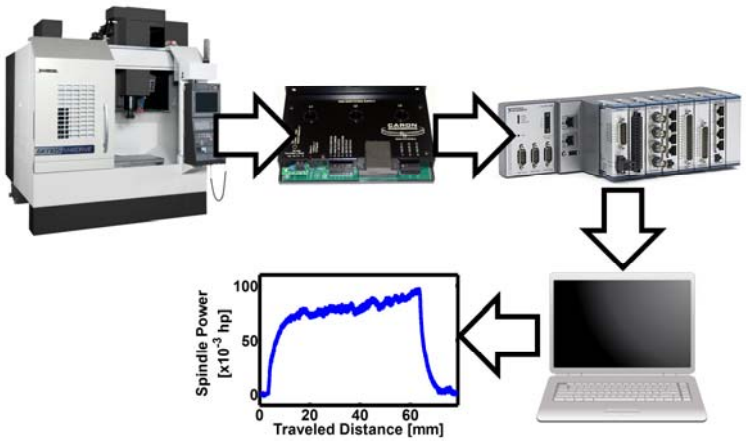

Inserts used in this work were Sandvik Coromill R390-11 T3 08M-PM 1030, hereafter referred to as '1030'. The 1030 grade (TiAlN PVD coated) is recommended by Sandvik for milling R-108 and similar difficult-to-machine materials due to its resistance to material build-up on the cutting edge and plastic deformation (Sandvik, 2006). Fresh unworn inserts were used at the beginning of each set of tests (eight passes), with Olympus optical microscope to measure flank wear on the bottom edge of insert. The progress of tool flank wear is shown in Figure 9 for tests 1.2, 1.4, 1.6 and 1.8 (first replication). Spindle power consumption was measured in 5 cutting distances (shown with '×' marker in Figure 7), each around 10, 20, 30, 40 and 50 mm. In Figure 10, an exemplified description of the smoothed spindle cutting power is shown for test 1.3. Measured power and tool flank of all the three replications set are shown in Table 1. Note that only the fifth spindle power measurement, i.e. P_5 as the spindle power consumption around 50 mm, is shown in Table 1.

Figure 9 Measured flank wear for (a) test 1.2, (b) test 1.4, (c) test 1.6, and (d) test 1.8 (see online version for colours)

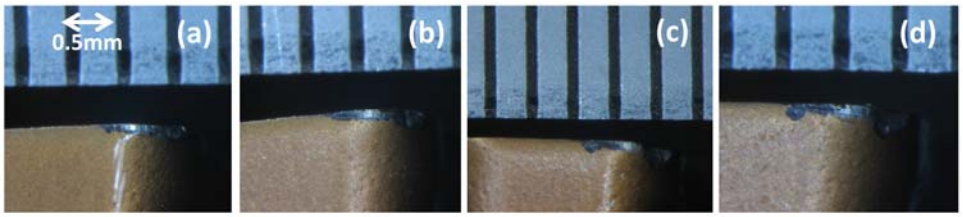

Figure 10 Smoothed cutting power for test 1.3 (see online version for colours)

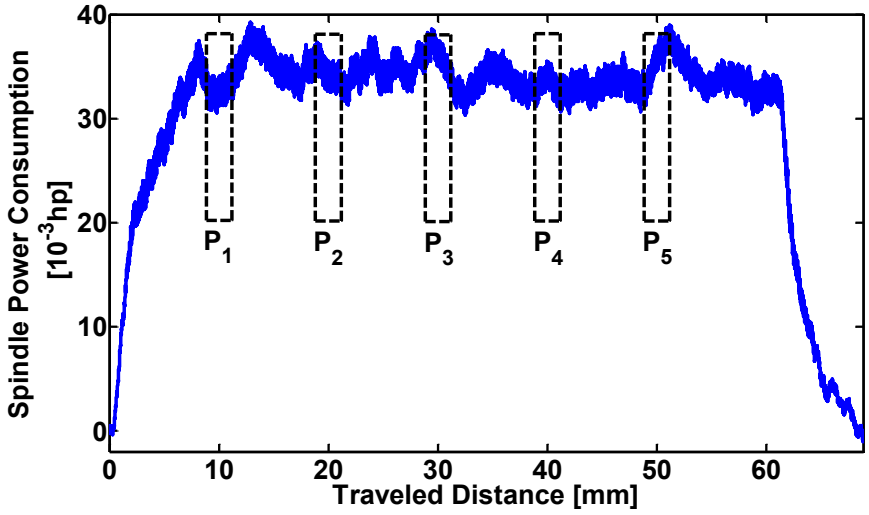

Table 1 Spindle power and flank wear measurement for training and testing sets

(a) Training sets						*(b) Testing set*		
Replication 1			*Replication 2*			*Replication 3*		
Test #	P^5 (10^{-3} hp)	*VB* (μm)	*Test* #	*P5* (10^{-3} hp)	*VB* (μm)	*Test* #	*P5* (10^{-3} hp)	*VB* (μm)
1.1	29	84	2.1	32	83	3.1	32	81
1.2	32	89	2.2	36	87	3.2	33	87
1.3	24	100	2.3	38	103	3.3	35	99
1.4	33	108	2.4	37	107	3.4	34	103
1.5	36	111	2.5	44	109	3.5	39	109
1.6	41	116	2.6	30	116	3.6	38	115
1.7	37	119	2.7	41	125	3.7	36	116
1.8	36	125	2.8	44	127	3.8	42	120

5 Stochastic modelling of tool flank wear

The dynamic behaviour of tool wear is nonlinear at the initial stages, linear at intermediate stages, and nonlinear at the final stages before catastrophic failure (Koren et al., 1991). Due to the high strength and hardness of R-108, the progress of tool wear was relatively fast, and the first stages of tool wear were not captured while testing. Hence, tool wear progress was considered as a linear function of volume of material removed (MR) while machining. Linear regression was used to find the slope of tool wear curves for each replication as shown in Figure 11. R_{adj}^2 values of 91%, 93%, and 87% for the three replications of the tests validate the aforementioned linear tool wear assumptions. Note that spindle power consumption was calculated in five regions during the process. However, tool wear are only available after each pass. To compensate the inconsistency between number of data points – $5 \times 8 \times 3 = 120$ points for spindle power and $8 \times 3 = 24$ points for tool wear– extra data points were interpolated, and Gaussian noise with zero mean and variance equal to 1.36×10^2 μm^2 were added to the interpolation to include uncertainties in measurements. The variances of tool wear were selected based on maximum variance of passes in each three sets of experiments [equation (27)].

$$\sigma_{tool\ wear}^2 = \max\left\{ \operatorname{var}\begin{pmatrix}1.1\\2.1\\3.1\end{pmatrix}, \operatorname{var}\begin{pmatrix}1.2\\2.2\\3.3\end{pmatrix}, \ldots, \operatorname{var}\begin{pmatrix}1.8\\2.8\\3.8\end{pmatrix} \right\}_{tool\ wear\ measurement} \tag{27}$$

Figure 11 Linear regression results of (a) replication 1, (b) replication 2 and (c) replication 3 (see online version for colours)

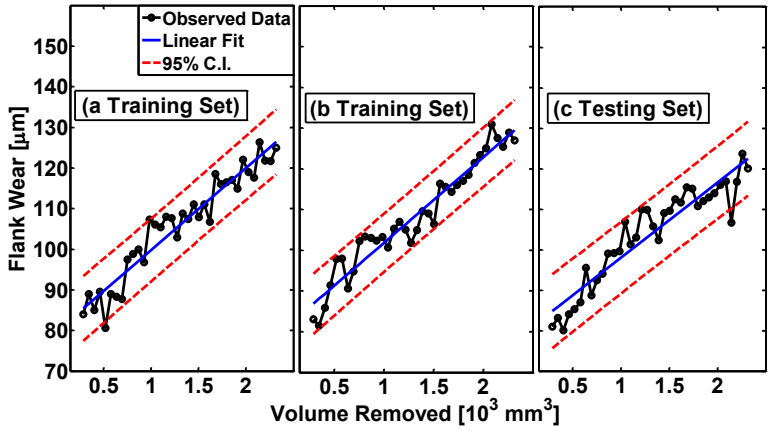

Considering the linear region for tool wear and assuming flank wear VB and slope of tool wear growth rate VB' as the states of the system, the discretised state space equation can be written as equation (28), where Δt is the time-step size. Assuming r_e as radial immersion, Δt can be written equivalent to the volume of removed material (MR) as $\Delta t = (120\pi D \times MR) / (f \times V \times a_p \times r_e)$. Because the cutting conditions were kept constant in this work, VB' can be defined as equations (28)–(29).

$$\frac{VB(k)-VB(k-1)}{\Delta t} = VB'(k) \rightarrow VB(k) = VB(k-1) + VB'(k)\Delta t \tag{28}$$

$$VB'(k) = VB'(k-1) \tag{29}$$

The state error should be included into the state equations as normally distributed noise. Note that error variances for tool wear and tool wear rate are assumed to be independent of one another. The stochastic state space equation is described in matrix format in equations (30)–(31).

$$\begin{bmatrix} VB(k) \\ VB'(k) \end{bmatrix} = \begin{bmatrix} 1 & MR \\ 0 & 1 \end{bmatrix} \begin{bmatrix} VB(k-1) \\ VB'(k-1) \end{bmatrix} + \begin{bmatrix} w_1(k) & 0 \\ 0 & w_2(k) \end{bmatrix} \tag{30}$$

$$\begin{bmatrix} w_1(k) \\ w_2(k) \end{bmatrix} \sim N\left(\begin{bmatrix} 0 \\ 0 \end{bmatrix}, \begin{bmatrix} Q_1 & 0 \\ 0 & Q_2 \end{bmatrix} \right) \tag{31}$$

The variance $Q_1 = 1.36 \times 10^2$ µm^2 was calculated based on the maximum variance in tool flank wear measurements between replications of tests and the variance $Q^2 = 1.6 \times 10^{-6}$ µm^2/mm^6 was calculated as the variance between slopes of linear regression curves. In all the experiments, cutting conditions were kept constant, so equation (26) can be simplified as a linear equation between spindle power consumption and tool wear [equation (32)].

$$P = K_{p1} + K_{p2} VB \tag{32}$$

The estimated value of K_{p1} and K_{p2} was already calculated in the previous work of authors based on general spindle cutting power model [equation (26)] using Bayesian parameter estimation method (Akhavan Niaki et al., 2015b). Moreover, linear regression analysis is used with the current training set to find K_{p1} and K_{p2} which is shown in Table 2. The difference in parameters is interpreted as uncertainties in parameters of the model due to the stochastic nature of the tool wear system.

Table 2 Comparison of Bayesian and linear regression estimation

Parameter	*Linear regression analysis*	*Bayesian parameter inference*
#	16 experiments	8 experiments
K_{p1}	17.9	15.8
K_{p2}	184.4	215.4

Spindle power consumption for each of three replications is shown in Figure 12. Measurement error variance for spindle power was calculated the same way as Q_1 as 11.3×10^{-3} hp^2. Equation (32) is written in discrete matrix format to run the Kalman filter as given in equation (33), where the measurement error $v(k)$ is defined as a normal distribution with zero mean and R covariance matrix. Note that, it is possible to tune the measurement errors and states error covariance based on the performance of the filter. By decreasing R, the effect of *a priori* will be strengthened on the estimations.

$$\Delta P(k) = \begin{bmatrix} K_{p2} & 0 \end{bmatrix} \begin{bmatrix} VB(k) \\ VB'(k) \end{bmatrix} + v(k) \tag{33}$$

$$v(k) \sim N(0, R) \tag{34}$$

Figure 12 Spindle power, (a) training set 1 (b) training set 2 (c) testing set 3 (see online version for colours)

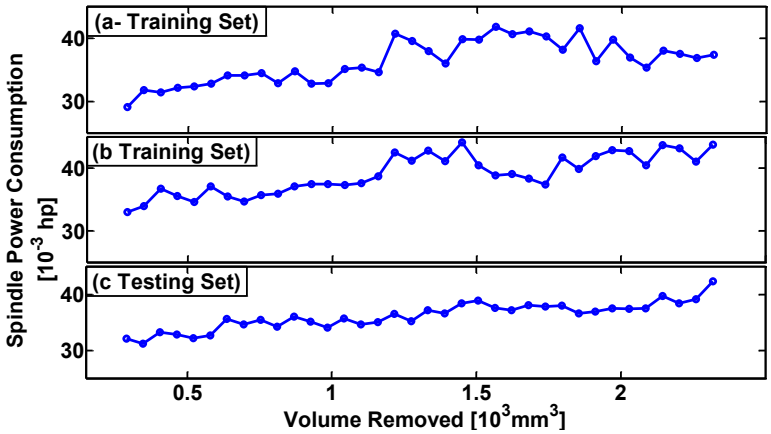

To run the Kalman filter, an initial point and an initial covariance for the states are required. The initial point (x_0) was calculated simply as the mean of predicted flank wear from test 1.1, 2.1, and 3.1. To find the initial error of the flank wear, the error between the mean of measured flank wear for first tests of each replication which appears as expected value of $VB_{i,1}$ in equation (35) and estimated flank wear based on measured

power which appears as expected value of $\Delta P_{i,1}/K_{p2}$ was calculated. The error of flank wear rate was calculated as the difference between the slope of measured flank wear [first term in equation (36)] and predicted flank wear using test sets (1.1, 1.2 and 1.3) and (2.1, 2.2 and 2.3) for each replication [second term in equation (36)]. Combining these two errors together, the initial error covariance of tool wear and tool wear rate were 4.8 μm and 7.7 $\mu m^2/mm^3$ respectively.

$$e_0 = E\left(VB_{i,1}\right) - E\left(\frac{\Delta P_{i,1}}{C_2}\right) i \in \{1, 2, 3\} \tag{35}$$

$$e_0' = E\left(\frac{VB_{i,1} - VB_{i,2}}{MR}\right) - E\left(\frac{P_{i,1} - P_{i,2}}{C_2 MR}\right) i \in \{1, 2, 3\} \tag{36}$$

$$P_0 = \begin{bmatrix} e_0 & e_0' \end{bmatrix} \begin{bmatrix} e_0 \\ e_0' \end{bmatrix} = \begin{bmatrix} e_0^2 & e_0 e_0' \\ e_0 e_0' & e_0'^2 \end{bmatrix} \tag{37}$$

To run Particle filter initial random samples from the initial distribution of states is required. Therefore, a thousand random samples (i.e. particles, N_s) with equal weights were drawn from the initial pdf of states (x) assuming a Gaussian pdf with mean of x_0 and variance Q.

$$x_0^i \sim N\left(x_0, Q\right) \quad i = 1, \ldots, N_s \tag{38}$$

$$\omega_0^i = \frac{1}{N_s} = 0.001 \quad i = 1, \ldots, N_s \tag{39}$$

Figure 13 Linear deterministic regression for tool flank wear estimation using spindle power measurement (see online version for colours)

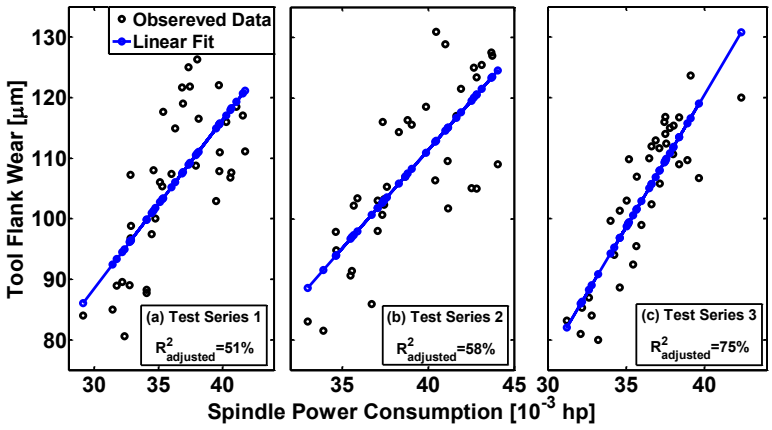

Before proceeding to the next section, it worth considering only the deterministic measurement model [equation (32)] with linear regression analysis and study its performance for tool flank wear estimation. The linear curve fit and corresponding

$R^2_{adjusted}$ as goodness of fit is shown in Figure 13. According to this figure, the 0.51, 0.58 and 0.75 values of $R^2_{adjusted}$ shows a weak linear relation between measurement and tool flank wear which can be due to low signal to noise ratio of power measurement and incompleteness of measurement model. This can be compensated by adding the state model [equation (30)] to the measurement model [equation (33)] and use filtering described methods to reduce the effect of noise.

6 Results using Kalman filter

Using the results of the regression analysis (Table 2) and assuming a deterministic value for spindle power parameters, tool flank wear estimation and the corresponding 95% confidence intervals are calculated from the estimated covariance (P_{cov}) for the training set and the testing set (Figure 14). Minimising the error between the measurements and predictions is the goal; therefore the measurement error covariance (R) and the state covariance (Q) were fine-tuned. The training sets and testing set resulted in average estimation errors of 11, 8, and 6%, respectively. The Kalman filter resulted in less than 17% estimation error for the testing set when spindle power consumption was used as the measurement signal (Figure 14). The shape of the flank wear evolution graph was not successfully captured with the filter, which is due to the effect of measurements. Theoretically, the spindle power consumption should be a monotonically increasing signal with increasing tool wear. Considering the training set 1 and 2 in Figure 12, there is an increase and then a decrease in the spindle power signal; so the curves are not monotonically increasing. This change in power is due to the initiation and progress of crater wear on the contact surface of inserts. First, the crater wear formation (beginning with test 4) reduces the spindle power temporarily. Then, spindle power increases with the progress of flank wear, and it keeps increasing afterwards. Moreover, a linear model is assumed for the process framework, but tool wear is a complex non-stationary dynamic process, and linear models may not fully represent the complex dynamics of tool wear.

Figure 14 Kalman filter flank wear estimation and its error for [(a) and (b)] training set 1, [(c) and (d)] training set 2 and [(e) and (f)] testing series 3 (see online version for colours)

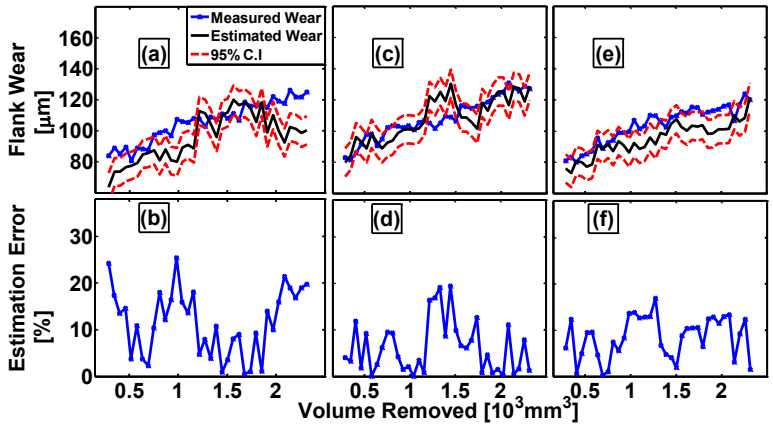

7 Results using particle filter

As stated in Section 6, the ability to characterise non-Gaussian distributions is one of the main advantages of the Particle filter over the Kalman filter. Considering the fact that using different parameter estimation methods (i.e. Bayesian parameter estimation and linear regression) for identifying the unknown parameters of spindle power model yields to two different values for the parameter K_{p2} (Table 2), a non-informative prior such as the uniform distribution or an informative prior such as a mixture of Gaussian distributions can be chosen as the initial pdf of the parameter K_{p2}. The initial pdf is then propagated and updated through the system update at each time step. Consequently, the next time step uses the updated pdf of the parameter as its initial pdf.

A uniform distribution is modelled around the minimum and maximum values of K_{p2} (Table 2) from 150×10^{-3} to 240×10^{-3} hp/μm. In modelling of Gaussian mixture, since results from the regression analysis were based on 16 experiments and is twice the number of total experiments from the Bayesian inference, it was assumed that confidence in accuracy of the results of the regression analysis is twice the confidence in accuracy of the results of Bayesian inference. Therefore, the Gaussian mixture is modelled with 2/3 weight for the coefficient that is derived using the linear regression analysis (16 experiments) and 1/3 weight for the coefficient that is derived using Bayesian parameter estimation (eight experiments). The mean of Gaussian mixture model is on 184×10^{-3} and 215×10^{-3} hp/μm with equal variances of 50×10^{-6} hp^2/μm^2. The combined parameter estimation and state estimation in Particle filter framework in the discrete state space format is rewritten as equations (40)–(41).

$$\begin{bmatrix} VB(k) \\ VB'(k) \end{bmatrix} = \begin{bmatrix} 1 & MR \\ 0 & 1 \end{bmatrix} \begin{bmatrix} VB(k-1) \\ VB'(k-1) \end{bmatrix} + \begin{bmatrix} w_1(k) & 0 \\ 0 & w_2(k) \end{bmatrix}$$

$$K_{p2} \propto \left(\frac{2}{3} N\left(184.4 \times 10^{-3}, 50 \times 10^{-6}\right) + \frac{1}{3} N\left(215.4 \times 10^{-3}, 50 \times 10^{-6}\right) \right) \tag{40}$$

or

$$K_{p2} \propto U\left(150 \times 10^{-3}, 250 \times 10^{-3}\right) \tag{41}$$

$$\Delta P(k) = \begin{bmatrix} K_{p2}(k) & 0 \end{bmatrix} \begin{bmatrix} VB(k) \\ VB'(k) \end{bmatrix} + v(k)$$

MC algorithm (Figure 15) was deployed to directly sample from the Gaussian mixture model of K_{p2} (Figure 16). By running Particle filter, at each time step k, the distribution of tool wear and the parameters K_{p2} become available. The mode of the posterior distribution is selected at each time step, and the result of estimation for the training and testing sets are shown in Figure 17 and Figure 18. Average estimation errors of 8% and 5% were observed for the testing set, assuming a uniform and a Gaussian mixture model, respectively. For a better performance comparison of Kalman filter and Particle filter, two error metrics (i.e. mean of estimation error and root mean square error) were computed (Table 3). It was observed that the Particle filter with bimodal initial prior pdf of spindle power coefficient is able to decrease the average error by of 33% and the root mean square error by 28% compared to Kalman filter. Note that the same pattern (non-monotonic progress of tool wear) was observed here as well.

Figure 15 Monte Carlo algorithm for drawing samples from Gaussian mixture model

- (0) FOR $i = 1{:}N_s$
  - Draw $u_i = Uniform(0, 1)$
- (1) IF $u_i < \frac{2}{3}$
  - Draw $K_{p1}^i \sim N(181.2, 50)$
- (2) ELSE
  - Draw $K_{p1}^i \sim N(215.4, 50)$
- END IF
- END FOR

Figure 16 Gaussian mixture prior pdf of K_{p2} (see online version for colours)

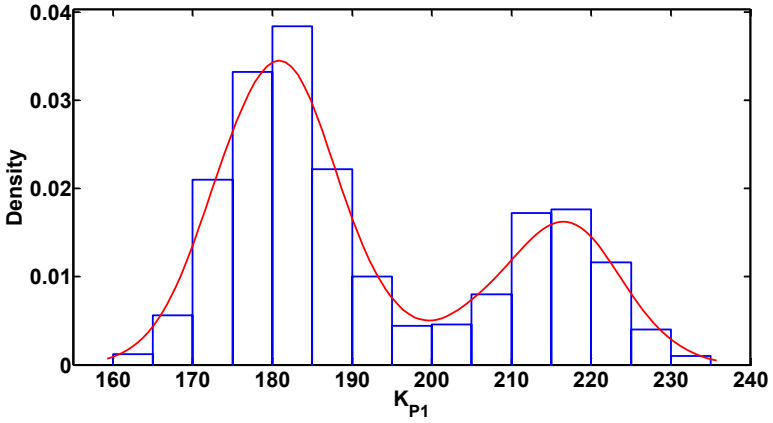

Figure 17 Particle filter flank wear estimation with uniform distribution of K_{p2} and its error for [(a) and (b)] training set 1, [(c) and (d)] training set 2 and [(e) and (f)] testing set 3 (see online version for colours)

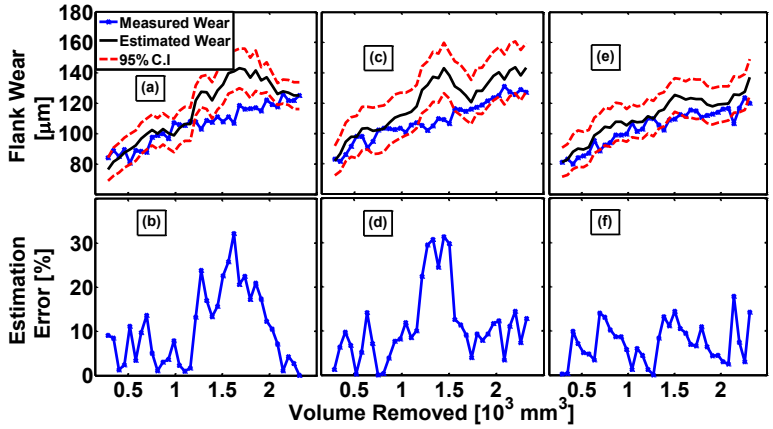

Figure 18 Particle filter flank wear estimation with Gaussian mixture distribution of K_{p2} error for [(a) and (b)] training set 1, [(c) and (d)] training set 2 and [(e) and (f)] testing set 3 (see online version for colours)

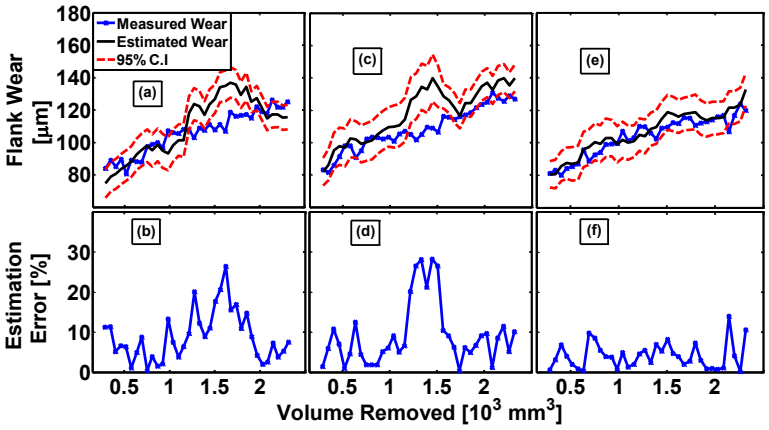

Table 3 Comparison of Kalman filter and Particle filter estimation error

Replication	*Kalman filter*		*Particle filter*			
			Uniform initial		*GMM initial*	
	E[error]	*RMSE*	*E[error]*	*RMSE*	*E[error]*	*RMSE*
Training set 1	11	13	11	15	9	12
Training set 2	8	12	11	15	9	13
Testing set 3	6	7	8	10	4	5

Figure 19 Evolution of K_{p2} through time from uniform model to unimodal model (see online version for colours)

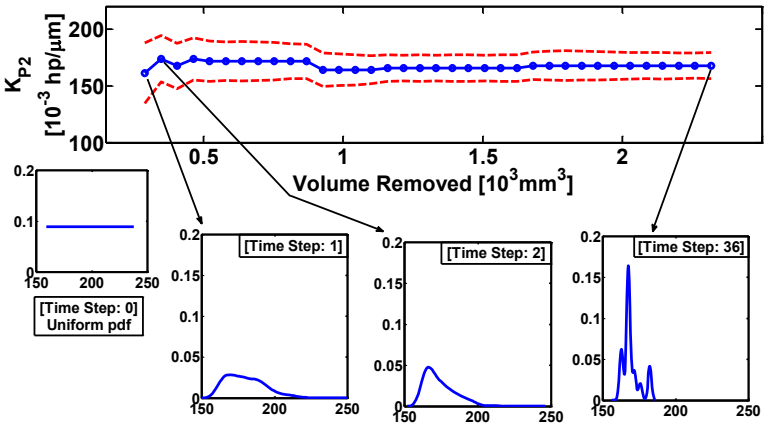

Figure 20 Evolution of K_{p2} through time from the bimodal to the unimodal Gaussian model (see online version for colours)

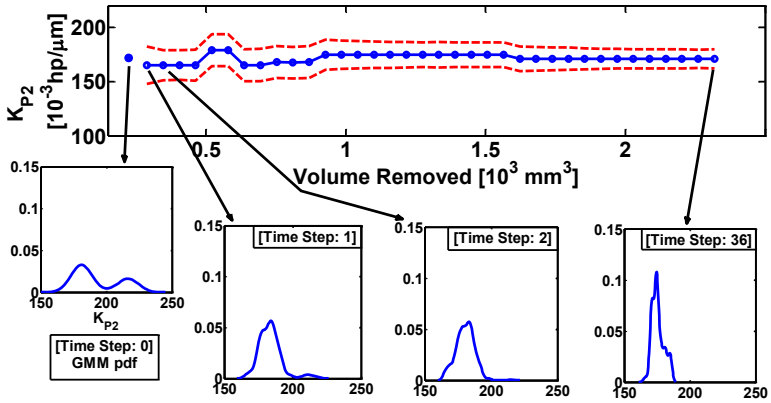

The evolution of K_{p2} with two different prior assumptions is shown in Figure 19 and Figure 20. Note that every point in those figures is a distribution (not necessarily Gaussian) that is characterised by Ns particles generated on each time-step. Intuitively, the bimodal Gaussian model cannot be a valid distribution for a parameter; however it can be a good initial estimate for the prior distribution, considering the fact that two different values were reported for this parameter. After continuing a few steps, the bimodal model and the uniform model change into a unimodal Gaussian model with averages of 0.17 hp/µm and 0.167 hp/µm for each different prior assumption.

8 Conclusions

In this study, a linear optimal estimation method (i.e. Kalman filter) and a SMC method (i.e. Particle filter) were used for tool flank wear estimation in end milling of gamma-prime strengthened difficult-to-machine alloys. Tracking tool wear in modern manufacturing processes is critical due to the fact that it can reduce downtime of the machine and increase productivity simultaneously. Spindle power consumption was used as the observed signal due to the low cost and easy implementation of Eddy current sensors in CNC machines used in real-life applications. The main conclusions of this study are given as below:

- Two types of stochastic filters were used within a discrete linear mechanistic tool wear model. Spindle power consumption signals were captured by a high frequency DAQ system, when relatively mild machining conditions were applied.
- State and measurement error variances were properly identified and the least possible estimation error was obtained by fine-tuning the Kalman filter. Through this fine-tuning, tool flank wear was estimated with a maximum error of 25% in the training set, and an average error of 6% in the testing set.
- Particle filter was also used for tool wear estimation, and its results were compared to estimation using Kalman filter. It was shown that using Particle filter, the estimation error decreased up to 33%.

- In addition to estimating tool wear, Particle filter was used for online estimation of the spindle power model coefficient. Uniform model and Gaussian mixture model were assumed as the initial pdf of the unknown parameter and their evolution with respect to time was investigated. It was shown that both models turn into the unimodal model after a few iterations with significant reduction in uncertainties in distribution of parameter at the final step.

Linear analytical models of spindle power in the context of a physics-based method were used in this work. However, linear models do not fully capture the nonlinear and complex essence of tool wear. Furthermore, other signals such as cutting force and vibration can be fused with spindle cutting power, and nonlinear models that better capture the dynamic behaviour of tool wear can be used instead of the linear models for relating flank wear to the observed signal. Data driven methods such as artificial neural networks (ANN) that have shown good performance in highly nonlinear and noisy systems can be an alternative to the physics-based techniques specifically for studying hard-to-machine materials. By using these methods, in addition to time series features of the power signal, other features in frequency or time-frequency domains can be related to tool wear. However, proper selection of signal features is critical because these features should be as insensitive as possible to changes in cutting conditions and highly sensitive to tool wear in order to have valid estimations under different machining conditions. Studying these features in machining difficult-to-machine materials is left for future studies.

Acknowledgements

The authors wish to thank the National Science Foundation for support of this work under Grant No. 0954318. Any opinions, findings, and conclusions or recommendations expressed in this material are those of the authors and do not necessarily reflect the views of the National Science Foundation.

References

Akhavan Niaki, F., Ulutan, D. and Mears, L. (2015a) 'In-process tool flank wear estimation in machining gamma-prime strengthened alloys using Kalman filter', *43rd North American Manufacturing Research Conference*.

Akhavan Niaki, F., Ulutan, D. and Mears, L. (2015b) 'Parameter estimation using Markov chain Monte Carlo method in mechanistic modeling of tool wear during milling', *ASME 2015 International Manufacturing Science and Engineering Conference*, American Society of Mechanical Engineers.

Altintas, Y. and Yellowley, I. (1989) 'In-process detection of tool failure in milling using cutting force models', *Journal of Manufacturing Science and Engineering*, Vol. 111, No. 2, pp.149–157.

Andrieu, C., De Freitas, N., Doucet, A. and Jordan, M.I. (2003) 'An introduction to MCMC for machine learning', *Machine Learning*, Vol. 50, Nos. 1–2, pp.5–43.

Arulampalam, M.S., Maskell, S., Gordon, N. and Clapp, T. (2002) 'A tutorial on particle filters for online nonlinear/non-Gaussian Bayesian tracking', *IEEE Transactions on Signal Processing*, Vol. 50, No. 2, pp.174–188.

Choudhury, S. and Rath, S. (2000) 'In-process tool wear estimation in milling using cutting force model', *Journal of Materials Processing Technology*, Vol. 99, No. 1, pp.113–119.

Cuppini, D., D'errico, G. and Rutelli, G. (1990) 'Tool wear monitoring based on cutting power measurement', *Wear*, Vol. 139, No. 2, pp.303–311.

Danai, K. and Ulsoy, A.G. (1987a) 'An adaptive observer for on-line tool wear estimation in turning, part I: theory', *Mechanical Systems and Signal Processing*, Vol. 1, No. 2, pp.211–225.

Danai, K. and Ulsoy, A.G. (1987b) 'An adaptive observer for on-line tool wear estimation in turning, part II: results', *Mechanical Systems and Signal Processing*, Vol. 1, No. 2, pp.227–240.

Doucet, A., De Freitas, N. and Gordon, N. (2001) *An Introduction to Sequential Monte Carlo Methods*, Springer, New York.

Ertunc, H.M., Loparo, K.A. and Ocak, H. (2001) 'Tool wear condition monitoring in drilling operations using hidden Markov models (HMMs)', *International Journal of Machine Tools and Manufacture*, Vol. 41, No. 9, pp.1363–1384.

Fu, H.J., DeVor, R.E. and Kapoor, S.G. (1984) 'A mechanistic model for the prediction of the force system in face milling operations', *Journal of Manufacturing Science and Engineering*, Vol. 106, No. 1, pp.81–88.

Haykin, S.S. (2001) *Kalman Filtering and Neural Networks*, Wiley Online Library.

Henderson, A. (2012) *Updated Force Model for Milling Nickel-based Superalloys*, Doctoral Dissertation, Clemson University.

Hoff, P.D. (2009) *A First Course in Bayesian Statistical Methods*, Springer Science and Media.

Imtiaz, S.A., Roy, K., Huang, B., Shah, S.L. and Jampana, P. (2006) 'Estimation of states of nonlinear systems using a particle filter', *IEEE International Conference on Industrial Technology, 2006, ICIT 2006*, IEEE, p.2432.

Jeon, J. and Kim, S. (1988) 'Optical flank wear monitoring of cutting tools by image processing', *Wear*, Vol. 127, No. 2, pp.207–217.

Kalman, R.E. (1960) 'A new approach to linear filtering and prediction problems', *Journal of Fluids Engineering*, Vol. 82, No. 1, pp.35–45.

Kitagawa, G. (1996) 'Monte Carlo filter and smoother for non-Gaussian nonlinear state space models', *Journal of Computational and Graphical Statistics*, Vol. 5, No. 1, pp.1–25.

Koren, Y., Ko, T., Ulsoy, A.G. and Danai, K. (1991) 'Flank wear estimation under varying cutting conditions', *Journal of Dynamic Systems, Measurement, and Control*, Vol. 113, No. 2, pp.300–307.

Li, X. (2002) 'A brief review: acoustic emission method for tool wear monitoring during turning', *International Journal of Machine Tools and Manufacture*, Vol. 42, No. 2, pp.157–165.

Lin, S. and Yang, R. (1995) 'Force-based model for tool wear monitoring in face milling', *International Journal of Machine Tools and Manufacture*, Vol. 35, No. 9, pp.1201–1211.

Möhring, H., Litwinski, K. and Gümmer, O. (2010) 'Process monitoring with sensory machine tool components', *CIRP Annals-Manufacturing Technology*, Vol. 59, No. 1, pp.383–386.

Owsley, L.M., Atlas, L.E. and Bernard, G.D. (1997) 'Self-organizing feature maps and hidden Markov models for machine-tool monitoring', *IEEE Transactions on Signal Processing*, Vol. 45, No. 11, pp.2787–2798.

Pedersen, K.B. (1990) 'Wear measurement of cutting tools by computer vision', *International Journal of Machine Tools and Manufacture*, Vol. 30, No. 1, pp.131–139.

Rawlings, J.B. and Bakshi, B.R. (2006) 'Particle filtering and moving horizon estimation', *Computers and Chemical Engineering*, Vol. 30, No. 10, pp.1529–1541.

Roth, J.T., Djurdjanovic, D., Yang, X., Mears, L. and Kurfess, T. (2010) 'Quality and inspection of machining operations: tool condition monitoring', *Journal of Manufacturing Science and Engineering*, Vol. 132, No. 4, p.041015.

Sandvik, C. (2006) *Steel Milling Stars, GC4240 and GC1030, C-1140, A Pair of Grades that Won't Crack Under Pressure*, Sandvik Company, Alachua, FL.

Shao, H., Wang, H.L. and Zhao, X.M. (2004) 'A cutting power model for tool wear monitoring in milling', *International Journal of Machine Tools and Manufacture*, Vol. 44, No. 14, pp.1503–1509.

Vallejo Jr., A.G., Nolazco-Flores, J.A., Morales-Menéndez, R., Sucar, L.E. and Rodríguez, C.A. (2005) 'Tool-wear monitoring based on continuous hidden Markov models', *Progress in Pattern Recognition, Image Analysis and Applications*, pp.880–890, Springer, Berlin, Heidelberg.

Waldorf, D.J., Kapoor, S.G. and DeVor, R.E. (1992) 'Automatic recognition of tool wear on a face mill using a mechanistic modeling approach', *Wear*, Vol. 157, No. 2, pp.305–323.

Wan, E.A. and Van Der Merwe, R. (2000) 'The unscented Kalman filter for nonlinear estimation', *Adaptive Systems for Signal Processing, Communications, and Control Symposium 2000, AS-SPCC, The IEEE 2000*, IEEE, p.153.

Wang, L., Mehrabi, M.G. and Kannatey-Asibu, E. (2002) 'Hidden Markov model-based tool wear monitoring in turning', *Journal of Manufacturing Science and Engineering*, Vol. 124, No. 3, pp.651–658.

Xu, C., Xu, T., Zhu, Q. and Zhang, H. (2011) 'Study of adaptive model parameter estimation for milling tool wear', *Strojniški vestnik-Journal of Mechanical Engineering*, Vol. 57, Nos. 7–8, pp.568–578.

Zhu, K., Wong, Y.S. and Hong, G.S. (2009) 'Multi-category micro-milling tool wear monitoring with continuous hidden Markov models', *Mechanical Systems and Signal Processing*, Vol. 23, No. 2, pp.547–560.

Nomenclature

α_{1-2}	Feedrate and depth of cut exponents	A	Process matrix relating states
a_p	Depth of cut (mm)	B	Process matrix relating control input and states
c	Chip thickness exponent	C_1–C_3	Constants
e_0	Initial error of tool wear (μm)	D	Cutter diameter (mm)
e_0'	Slope of initial error (μm/mm^3)	F_t	Tangential force (N)
f	Feedrate (mm/rev)	F_t^{wear}	Tangential force due to tool wear (N)
$\overline{h}$	Mean chip thickness (mm)	H	Matrix relating states and measurements
k	Time step	H_h	Material hardness
m	Number of cutter tooth	K	Kalman gain
r_e	Radial immersion	Kp_{1-2}	Simplified power model coefficients
s	Tool wear length (mm)	K'	Specific cutting pressure per tooth
u	Control input	K_1–K_3	Spindle power model constants
q	Proposal density function	MR	Volume of removed material (mm^3)
v	Measurement noise	N	Spindle speed (rpm)
w	Process noise	N_{eff}	Effective number of particles
x	Stochastic event/state	N_s	Number of particles
x_0	Initial value of states	P	Cutting power (hp)
$\hat{x}^-$	*A priori* estimate of states	P^-	*A priori* error covariance of states
$\hat{x}$	*A posteriori* estimate of states	P'	*A posteriori* error covariance of states
y	Observation	Q	Process noise covariance

Nomenclature (continued)

z	Measurement signal	R	Measurement noise covariance
$\delta(x)$	Dirac delta function	R_{adj}^2	Goodness of fit
ε	Measurement error	VB	Tool flank wear (μm)
λ_s	Rake angle	VB'	Slope of tool flank wear (μm/mm^3)
μ	Friction coefficient	Δt	Time step increment (sec)
ω	Particles' weight		
$\pi(x)$	Prior function		
φ	Instantaneous angle of rotation		
ψ	Insert angle		
ψ_{1-2}	Entrance and exit immersion angle		